Rapid thermal oxidation of silicon in ozone

Zhenjiang Cui, Jonathan M. Madsen, and Christos G. Takoudis[a)]
Department of Chemical Engineering, University of Illinois at Chicago, Chicago, Illinois 60607

(Received 28 October 1999; accepted for publication 28 February 2000)

Rapid thermal oxidation (RTO) of Si in ozone gas is studied at temperatures between 200 and 550 °C, and the properties of the resulting ultrathin oxides are characterized using *in situ* mirror-enhanced reflection Fourier transform infrared (IR) spectroscopy. Thus, the frequency and intensity of the longitudinal optical vibrational mode of the Si–O–Si asymmetric stretching from ultrathin oxide films (<30 Å) are probed in different processing environments and related to the oxidation kinetics and interfacial layer properties. The oxidation rate in ozone is found to be comparable to the one in pure oxygen at approximately 200 °C higher temperature. Analyses of the oxidation in ozone show a fast oxidation regime followed by a slow one with activation energies of 0.13 ± 0.01 and 0.19 ± 0.04 eV, respectively. Two regions are also observed for the oxidation in pure O_2 with activation energies of 0.20 ± 0.03 eV for the fast oxidation regime and 0.36 ± 0.04 eV for the slow one. X-ray photoelectron spectroscopy results and IR spectral feature frequency shifts suggest that the RTO of silicon in ozone ambient results in a thinner, less-stressed interfacial layer than the one obtained in pure O_2. Preliminary electrical characterization using surface charge analyses indicates that the oxides formed in ozone are of superior quality. © *2000 American Institute of Physics.* [S0021-8979(00)06411-2]

I. INTRODUCTION

While the dimensions of integrated circuits are continuously shrinking, ultrathin (<30 Å) SiO_2 films for gate oxide applications or gate oxide precursors formed at relatively low temperatures (<600 °C) are becoming more important. To overcome low growth rates in that temperature range, ozone appears to become a promising substitute to oxygen for semiconductor surface oxidations. Further, there has been interest in the physical and chemical properties of this ''ozone oxide.''[1–4]

In practice, there are two general reactor configurations used to directly oxidize Si in ozone gas. The first is often referred to as ultraviolet (UV) light assisted ozone oxidation,[1,5] and it consists of UV lamps that shed light directly on the wafer; ozone is thus generated from the interaction of the UV light ($\lambda<200$ nm) with O_2. The second one is to generate ozone gas upstream the oxidation system and feed it into the oxidation chamber.[3,6] The former configuration seems to have higher oxidation rates than the latter. However, for UV-assisted ozone oxidation, an additional lamp system must be added to the top of the processing chamber, which, in most rapid thermal processing (RTP) systems, may be occupied by either a heating lamp system or a pyrometer. In the latter configuration, ozone is generated in a chamber upstream the reactor by passing oxygen through an UV lamp system (~1% O_3) or through a barrier discharge ozonizer (~2%–10% O_3) and then fed into the main reactor chamber. In this study, we focus on the latter mode of operation.

Although large enhancements in the oxidation rate have been reported,[4–6] most of the ozone-based oxide films are significantly thicker than 30 Å. Results for films less than 30 Å are sparse, perhaps in part because resistive heating has mostly been used. Boyd and coworkers,[2] for example, studied ozone oxidation at 600–1200 °C with oxide thickness between 60 and 170 Å. Here, however, a RTP system is used to study ultrathin (<30 Å) SiO_2 films and their formation kinetics in ozone gas at the temperature range of 200–550 °C. Furthermore, process-property relationships of these oxides are probed with *in situ* mirror-enhanced reflection Fourier transform infrared (MER-FTIR) spectroscopy.

Spectral IR parameters such as peak frequency, width, and intensity can be related to physical and chemical properties of dielectric materials.[7–9] The shift of the longitudinal optical (LO) (~1250 cm^{-1}) and transverse optical (TO) (~1060 cm^{-1}) modes of Si–O–Si asymmetric stretching may reflect changes in both oxide composition and strain distribution. A systematic IR study of the ultrathin oxide growth in ozone ambient is needed.[5,10] The MER-FTIR we have developed to study process-property relationships of ultrathin films allows us to study *in situ* oxide IR spectral features at different processing environments, for oxides as thin as 3 Å. Using *in situ* data from MER-FTIR spectroscopy coupled with complementary information obtained from x-ray photoelectron spectroscopy (XPS), spectral ellipsometry, and surface charge analyzer (SCA), the ozone oxidation kinetics and properties of the oxides are obtained, presented, and discussed.

II. EXPERIMENT

Experiments were carried out in an 860 cm^3 RTP reactor, with heating rates of about 20 °C/s. The sample temperature was controlled within ±1 °C with a proportional-integral-differential controller. After the sample was loaded into the reactor chamber, the processing and IR monitoring

a)Author to whom correspondence should be addressed; electronic mail: takoudis@uic.edu

were finished before the sample was exposed to the ambient atmosphere. Ozone was produced in a custom-made UV based ozone generator containing low pressure Hg lamps, which emitted two main frequencies, 185 and 254 nm, at a relative intensity ratio of approximately 1:10. The inlet ozone concentration was measured and thus controlled at 950 ± 10 ppm using a model 450 ozone monitor (Advanced Pollution Inc.).

Double polished 4 in. *n*-Si(100) wafers were diced into 15 mm×22 mm samples to fit into the sample holder. All samples were first cleaned in Summa Clean (a mixture of choline and methanol) for 20 min at 40 °C to remove contamination, followed by a 30 s dip in buffered HF (NH_4F: 49%HF, 10:1) to remove the native oxide. Samples were rinsed in deionized water for 1 min after chemical processing. The HF treated oxide-free sample was loaded into the RTP system within 1 min and purged with Ar gas (99.995%). After that, the system was subjected to a flow of 1 slm O_3 (950 ppm)/O_2 for 3 min (i.e., about four reactor residence times) until the ozone concentration reached a steady value of 950 ppm within the reactor, prior to heating. Preliminary experiments showed that the 3 min exposure to O_3/O_2 purging at room temperature resulted in negligible oxidation of the silicon sample (also see next section). After the desired stable ozone concentration was reached, the sample was rapidly heated to the oxidation temperature. Following the oxidation period, the lamps were turned off and the system was immediately purged/cooled with Ar.

IR spectra of the substrate and gas phase species inside the reactor were collected before, during, and after heating. Data was collected using a Nicolet Magna 560 IR spectrometer with an MCT-A detector. *In situ* measurements were realized using a reflection absorption configuration through two KBr windows and a beam incidence angle of 73°. In order to get a distinct IR signal from thin SiO_2 films (as thin as 3 Å), a mirror-enhanced reflection configuration was used.[11] The mirror-enhanced mode allows the Si–O–Si asymmetric stretching LO mode intensity to increase by a factor of about 20 compared to the normal one (i.e., without mirror enhancement). The LO mode intensity has been found to increase linearly with the thickness of oxide films less than 30 Å thick. Film thickness was also measured and calibrated independently with a J. A. Woollam M-44 spectral ellipsometer operated at an incident angle of 75°.

Film thickness and properties of the oxide/Si interface were also studied with XPS using a physical electronics PHI 5400 XPS/UPS spectrometer equipped with a monochromatic Al $K\alpha$ source (1486.6 eV) and a hemispherical electron energy analyzer. All scans were performed with a pass energy of 37.5 eV and data was collected at 15°, 30°, and 90° takeoff angles. The thickness obtained from XPS was determined using the Si $2p$ intensity ratio of the oxidized silicon film, I_{oxy}, and unoxidized silicon, I_{Si}, by the well-established method

$$D_{oxy}=\lambda_{oxy}\sin\alpha\ln[I_{oxy}/(\beta I_{Si})+1],$$

where λ_{oxy} is the photoelectron mean free path in the oxide, α is the photoelectron take off angle, and β is the ratio of $I_{oxy,\infty}/I_{Si,\infty}$, which is determined by measuring thick thermal oxides and H-terminated Si (100) surfaces. In this study, λ_{oxy} and β were taken to be 29 and 0.82 Å, respectively.[12] The photoelectron intensities of each oxidation state were related to the number of atoms in each oxidation state in the manner suggested by Himpsel *et al.*,[13] and Lu and Graham.[12] Also, the fixed oxide charge density, Q_{ox}, and the density of interface traps, D_{it}, were determined using a model 2500 (SCA) at Semitest Inc. Details of this technique can be found in Ref. 14.

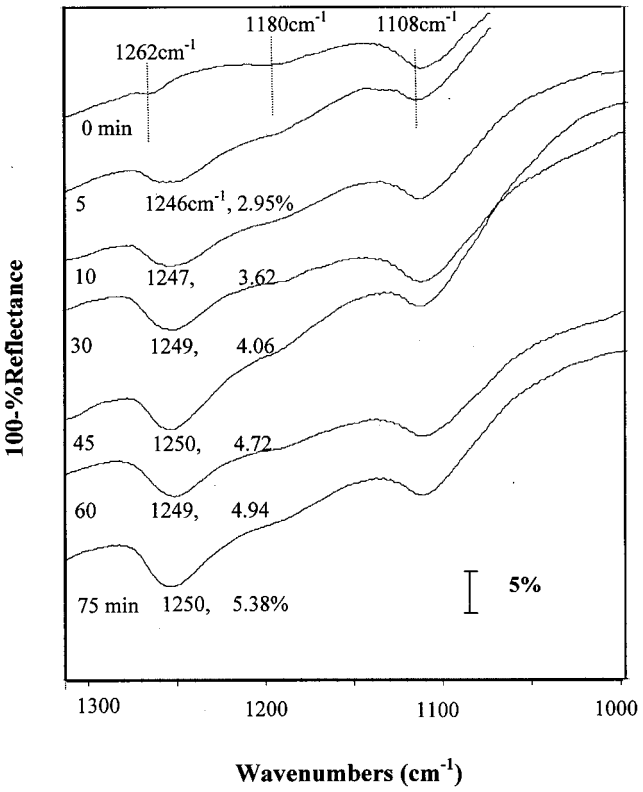

FIG. 1. *In situ* reflection IR spectra (1000–1300 cm^{-1}) obtained with the mirror-enhanced mode (Ref. 11) for Si (100) oxidized in O_3 (950 ppm)/O_2 at 400 °C and 1 slm total feed flow rate. The sample was heated in the RTP reactor starting with a hydrogen-terminated oxide free surface. The total oxidation time is 75 min.

III. RESULTS AND DISCUSSION

Figure 1 shows typical IR spectra (1000–1300 cm^{-1}) of Si (100) oxidized at 400 °C in O_3 (950 ppm)/O_2. Beginning with a H-terminated oxide free surface, the Si sample was oxidized for a total time of 75 min. During the oxidation process, IR spectra were obtained using both P and S-polarized light. The P-polarized spectra contain both the LO and TO modes of the Si–O–Si asymmetric stretching, while the S-polarized spectra contain only the TO mode.[11,15] After background correction (i.e., using the S-polarized spectrum as the background), only the LO feature (1245–1250 cm^{-1}) remains. Three other peaks also appear in the IR spectra (Fig. 1). The band at 1108 cm^{-1} was assigned to the interstitial oxygen in the bulk Si. Additional experiments suggested that the other two small spectral features at 1180 and 1262 cm^{-1} (the intensity of which remains constant

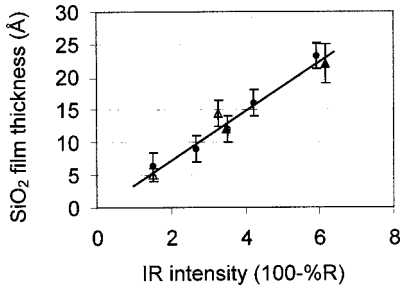

FIG. 2. Oxide film thickness vs *in situ* infrared intensity (100% reflectance) measured with MER-FTIR in both O_3 (950 ppm)/O_2 (closed symbols) and pure O_2 reactor feeds (open symbols). Thickness is obtained using XPS (triangular symbols) and spectral ellipsometry (circular symbols).

throughout the experiment) were due to the platinum mirror being used in the mirror-enhanced method.[11] Further, the IR spectra contain rather weak bands at about 2100 cm^{-1} (i.e., Si–H bonds), the intensity of which was too weak to allow detailed analyses.

As the oxidation in ozone proceeds, intensity changes and shifts in the peak position of the LO mode are probed (Fig. 1). After 5 min of oxidation at 400 °C, the intensity of the LO mode is $2.95\pm0.05\%$ with a frequency of 1246 ± 0.5 cm^{-1}. The LO peak intensity is seen to continuously increase with time up to 5.38% (after 75 min), while its peak position upshifts to about 1250 cm^{-1}. Spectra at different processing temperatures and in the same ozone ambient or in pure oxygen show similar trends (see below).

IR intensity represents the number of bonds and is not affected much by density changes.[16] Figure 2 shows the relationship of the LO mode intensity with the corresponding film thickness obtained through spectral ellipsometry and XPS. Samples have been heated to a temperature between 200 and 550 °C in either O_3 (950 ppm)/O_2 or pure O_2. It is seen that the MER-FTIR intensity (100-% reflectance) is linear with thickness in this temperature span. Additional experimental results, theoretical simulations, and explanation for this linear relationship are reported elsewhere.[11] Based on such findings, *in situ* IR intensity can be directly related to film thickness, at least for films thinner than 30 Å (Fig. 2).

Figure 3 shows the silicon oxide film thickness (via IR intensity) with time in the temperature range of 200–550 °C. The data shows an increase in the oxidation rate with temperature. Also, the Si (100) sample oxidation rate in ozone gas is seen to be substantially higher than that in pure oxygen; indeed, it is seen that the growth rates of ozone-oxidized samples are almost the same with the ones of pure O_2-oxidized substrates at about 200 °C higher temperature. In fact, the extent of the enhancement appears to vary with temperature and time. For example, during the first few minutes of oxidation, the ratio of the oxidation rate (thickness/time) in O_3 (950 ppm)/O_2 over the one in pure oxygen appears to increase from 2.65 at 300 °C to about 2.85 at 400 °C, but it starts decreasing above 400 °C to about 2.4 at 500 °C. Further, for longer times (up to 60 min), this ratio appears to decrease from 2.6 at 300 °C to about 2.0 at 500 °C. There seems to be a *turning point* between 400 and 500 °C, where the enhancement of the oxidation rate in the ozone gas over

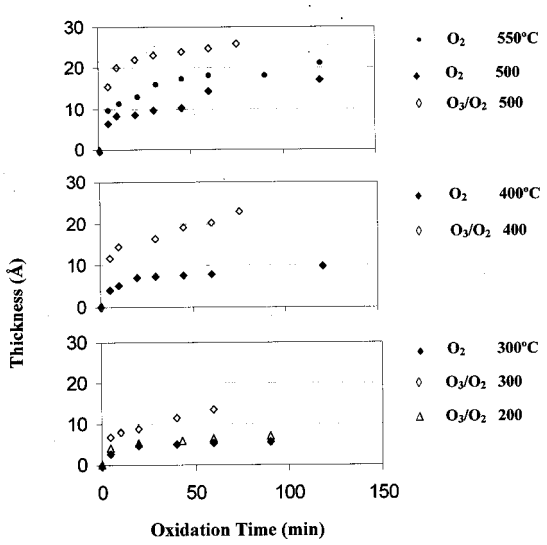

FIG. 3. Silicon oxide film thickness (obtained via *in situ* IR intensity) vs oxidation time in O_3 (950 ppm)/O_2 (◇ and △), and pure O_2 (◆ and ●), for a feed flow rate of 1 slm, at temperatures between 200 and 550 °C.

the one in pure oxygen begins to decrease. Similar enhancements have been reported at substantially higher temperatures (600 and 800 °C).[2,6,17] The change in the oxidation enhancement is most likely due to changes in the gas phase environment with increasing temperature. As the sample/substrate temperature increases, more ozone decomposes away from the sample surface due to the heating of the gas phase (also see below).[18] Therefore, as the temperature increases, the effective amount of ozone reaching the surface actually decreases. When less ozone reaches the sample surface, the enhancement of the oxidation rate decreases as the temperature increases. Because the amount of effective ozone reaching the surface is affected by many factors such as system geometry and kinetic parameters, the turning point mentioned above would be expected to be different from system to system.[2,6]

Another feature of the data is that there appears to be a fast initial oxidation rate regime followed by a slow one (Fig. 3). For instance, at 500 °C in O_3, it takes about 20 min to grow 22 Å (e.g., ~1 Å/min) of oxide, while 55 min more is required for an additional thickness of about 4 Å (e.g., ~0.07 Å/min). In all cases below, the oxidation rate is calculated based on zero oxide thickness at $t=0$ min. Indeed, after HF etching, the average contact angle of five samples was $75\pm1°$, which corresponded to fully H-terminated surface.[19] Also, several samples analyzed with spectral ellipsometry after the cleaning/etching procedure indicate that there is no oxide on the silicon surface. Similar results of two oxidation rate regimes were obtained[20] in microwave plasma afterglow oxidation where the oxidation rate was initially 2.1 Å/min, and it decreased to 0.5 Å/min after a 40–50 Å thick SiO_2 film was formed. The two different growth rates suggest that multiple physical/chemical phenomena are involved in the oxidation process. Assuming an Arrhenius temperature dependence for the different oxide growth regions,[21] Arrhenius plots are shown in Fig. 4; the corresponding activation energies are presented in Table I.

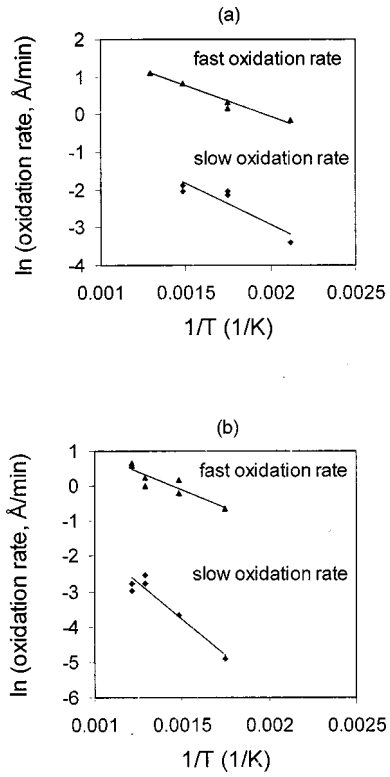

FIG. 4. Arrhenius plots of oxidation rates in O_3 (950 ppm)/O_2 (a) and pure O_2 (b). In both ambients, the top plot refers to the initial fast oxidation rate region, while the bottom one corresponds to the slow oxidation rate regime.

Based on the 5 min data, the initial activation energy for the ozone oxidation is calculated to be 0.13 ± 0.01 eV. This value is close to that of the electron cyclotron resonance oxidation (0.06–0.1 eV), where active atomic oxygen radicals are believed to be responsible for the rather small activation energy. The corresponding initial activation energy for the oxidation in pure O_2 is found to be 0.20 ± 0.03 eV, i.e., higher than that for O_3 and close to the activation energy of 0.3 eV for the second-layer oxidation in O_2.[22] Therefore, oxidation in O_3 is energetically more favorable than oxidation in pure O_2 oxidation; the apparent reduction in activation energy may be attributed to the presence of atomic oxygen radicals during the early stage of the ozone-based process.

As the substrate oxidation proceeds, the rate is seen to slow down while the activation energy for this ''slow oxidation rate regime'' increases to 0.19 ± 0.04 eV in O_3 (950 ppm)/O_2 ambient and 0.36 ± 0.04 eV in pure O_2. The relatively lower oxidation rate in ozone at 500 °C (Table I) may be *well after* the turning point of the oxidation rate enhancement in ozone discussed above.[18] Hence, this data point is not included in our data analysis. For a film less than 30 Å thick, isotope labeling studies[23,24] have indicated that there is a surface oxygen exchange region of about 10 Å, which overlaps with the near-interface oxidation region (10–40 Å). Therefore, during ozone oxidation, O_3 might prefer to dissociate into atomic oxygen on the substrate surface that would then transfer to the near-interface reacting region. Thus, the dissociation of O_3 on the substrate surface could be the rate-limiting step and its activation energy would be close to the one obtained for the oxidation process.[25]

To study the role of the gas phase chemistry, additional experiments were performed during the oxidation in an ozone environment. The O_3 gas phase concentration was probed by *in situ* FTIR spectroscopy at different temperatures. For a sample surface temperature of 530 °C, 75% of the inlet ozone was found to decompose at steady state, while at 125 °C, only 9.5% of the ozone fed into the system decomposed. Assuming a first order reaction, the dissociation activation energy obtained is about 0.17 eV, that is, a value close to the activation energy of 0.19 eV in the slow oxidation rate region. This suggests that in the case of oxidation in ozone for longer times, the rate-limiting step may be the ozone dissociation, while oxidation proceeds mainly via atomic oxygen. On the other hand, this is not the case during Si (100) oxidation in pure O_2 at temperatures below 550 °C, either in the fast or in the slow oxidation rate regime.

Oxide composition changes and strain distributions were investigated by probing frequency shifts of the LO mode of the Si–O–Si asymmetric stretching with oxidation time, substrate temperature, and reactor ambient, i.e., O_3/O_2 or pure O_2.[7–9] These data are shown in Fig. 5. For both environments, O_3/O_2 and pure O_2, increasing oxidation temperature or increasing processing time results in spectral frequency upshifts. At each temperature, the upshift is seen to be higher for shorter oxidation times, and it becomes negligible for longer oxidation times; further, the LO frequency of an ozone-oxidized sample is always seen to be higher than the one of a substrate processed in pure O_2.

The spectral frequency of the Si–O–Si asymmetric stretching vibrational mode shifts because of three main phe-

TABLE I. Rates and activation energies of rapid thermal oxidation in O_3 (950 ppm)/O_2 and pure O_2 gas. Data and results are presented for the fast oxidation regime during the first 5 min of the process (fast region), and the slow one after the first 20–30 min of the process (slow region).

	O_3/O_2 initial oxidation rate (fast region) Å/min	O_3/O_2 oxidation rate (slow region) Å/min	O_2 initial oxidation rate (fast region) Å/min	O_2 oxidation rate (slow region) Å/min
200 °C	0.85	0.03		
300 °C	1.4 (1.2[a])	0.12 (0.12[a])	0.53	0.0074
400 °C	2.3 (2.3[a])	0.13 (0.15[a])	0.81 (1.2[a])	0.026
500 °C	3.1	0.07[b]	1.3 (1.0[a])	0.081 (0.063[a])
550 °C			1.9 (1.9[a])	0.056 (0.063[a])
Activation energy (eV)	0.13 ± 0.01	0.19 ± 0.04	0.20 ± 0.03	0.36 ± 0.04

[a]Repeat runs.
[b]Not used in activation energy calculation (see text).

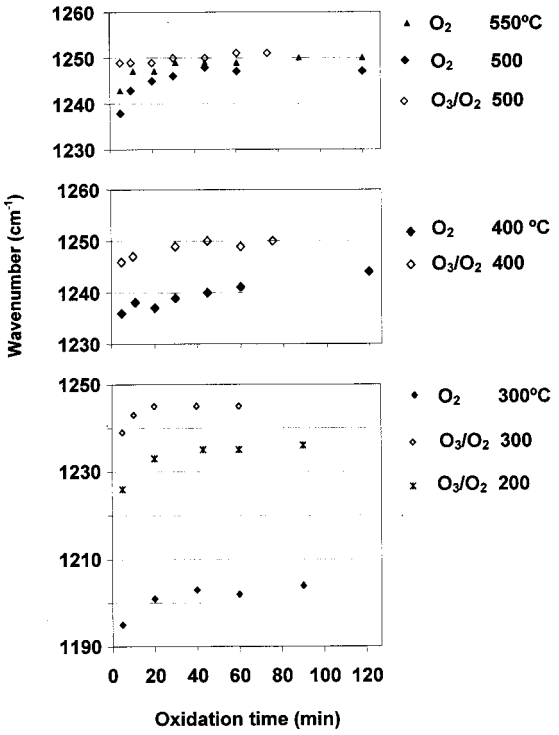

FIG. 5. Frequency shifts of the LO mode of Si–O–Si asymmetric stretching from ultrathin oxide films vs oxidation time in O_3 (950 ppm)/O_2 (◇ and ★) and pure O_2 (◆ and ▲) at a flow rate of 1 slm, and temperatures between 200 and 550 °C.

nomena. One is a change of the Si–O–Si bond angle, which decreases under the intrinsic compressive stress of a thermally grown oxide and results in a shift towards lower wave number.[9] When the temperature increases, the strain/stress decreases and thus the Si–O–Si bond angle increases, which in turn would result in an upshift of the LO and TO features. Changing stoichiometry of the oxide film is another source for shifts of the LO spectral frequency. Frequencies of suboxides, SiO_x ($x<2$), are lower than that of SiO_2; these substoichiometric oxides (or suboxides) are normally confined to a range of 5–15 Å from the interface.[7,8] Therefore, as silicon oxidation proceeds and the oxide becomes more ''bulk like'' (i.e., a stoichiometric oxide), the peak position of the Si–O–Si mode could shift to higher energies. Also, a very large thickness change, such as from 100 to 1000 Å can result in an upshift of the TO frequency up to 5 cm^{-1}. However, the LO frequency changes little with film thickness.[26] For the thickness range of our experiments, therefore, this effect would not be expected to be important at all.

In order to study the frequency shifts presented in Fig. 5, XP spectra were curve fitted using the methodology proposed by Lu *et al.*[12] for suboxide quantification. Table II shows the amount of suboxide species as functions of temperature. At 300 °C, ozone processing is found to reduce the suboxides from about 2 (in pure oxygen) to 1.6 ML, while at 500 °C from 1.7 (in pure oxygen) to 1.1 ML. This change in the amount of suboxides could account for, at least in part, the upshift of the LO mode of oxides formed in ozone when compared to the ones of oxides processed in pure O_2 (e.g., Ref. 27). As the oxidation temperature increases, the amount of suboxides is found to decrease for both ozone- and pure oxygen-processed samples. This is consistent with (i) the lower transition time to the near asymptotic value of the LO mode frequency at higher processing temperatures, and (ii) the smaller overall upshifts seen at high processing temperature (Fig. 5). Such results are in general agreement with the ones reported by Ono *et al.*,[7] and Madsen *et al.*[18]

TABLE II. Suboxide monolayers in oxide films formed at 300 and 500 °C in O_3 (950 ppm)/O_2 and pure O_2.

Oxidation temperature (°C)	300	300	500	500
Oxidant	O_2	O_3/O_2	O_2	O_3/O_2
Suboxide monolayers (ML)[a]	2.0	1.6	1.7	1.1

[a]ML defined as 6.78×10^{14} atoms/cm^2 (Ref. 12). The values of suboxide monolayers are the average data collected at 15°, 30°, and 90° takeoff angles.

Frequency shifts in the LO phonon of the Si–O–Si asymmetric stretching towards lower wave numbers are seen to take place less than about 8 ± 1 Å from the interface, which is also found to be the approximate thickness of the transition layer of the Si-rich suboxide layers. This differs from the value of 15 Å reported for relatively thicker films prepared at rather unspecified conditions and etched back using a dilute HF solution.[7] Different methods of substrate processing and preparation as well as the use of *ex situ* FTIR in Ref. 7 could account for such observed differences.

Fitch *et al.*[9] have reported TO frequency shifts for thicher films (>60 Å) processed at temperatures higher than 700 °C; these shifts have been suggested to be the result of stress and stress gradients at the SiO_2/Si interface. Also, those gradients are reported to be largest in films grown or annealed at temperatures in excess of 1050 °C. In this study, since the LO mode upshift at lower substrate temperatures is seen to be rather substantial, strain/stress in some films may be thought of as a partial contributor to the observed frequency shifts.[9,28] Yet, the fact that higher shift changes are observed at lower substrate temperatures (in fact, much lower than 700 °C), strain/stress contributions to the observed shifts would most likely be small, if any.

Figure 5 shows that the sample oxidized in ozone at 500 °C reached the asymptotic plateau in less than 5 min, with a thinner transition suboxide layer, 1.1 ML. Since the oxide has a thin interfacial layer and shows characteristics of bulk-like SiO_2 after only 5 min, high quality ultrathin oxide layers may indeed be realized using ozone oxidation. This is corroborated by capacitance–voltage measurements of the films using surface charge analyses. The oxide formed in ozone at 500 °C shows better electrical properties, i.e., less Q_{ox} ($4.9\times10^{10}\,q/\mathrm{cm}^2$) and lower D_{it} (3.7×10^{11} $\mathrm{eV}^{-1}\,\mathrm{cm}^{-2}$) than the oxide formed in pure oxygen at the same conditions ($Q_{ox}=5.7\times10^{11}\,q/\mathrm{cm}^2$ and $D_{it}=1.1\times10^{12}$ $\mathrm{eV}^{-1}\,\mathrm{cm}^{-2}$). These preliminary values for ozone gas processing agree well with and appear to be promising compared to those reported in the literature. Ishikawa *et al.*[29] have investigated oxidation of Si (100) in an O_2+UV environment at 500 °C for 1 hr and have achieved fixed oxide charge density and density of interface states of 3.8

$\times 10^{10}\, q/\mathrm{cm}^{-2}$ and $2\times 10^{12}\,\mathrm{eV}^{-1}\,\mathrm{cm}^{-2}$, respectively. Literature data for oxidation in O_2 at these low temperatures is not readily available. However, a fixed oxide charge density of $3.7\times 10^{11}\, q/\mathrm{cm}^{-2}$ and a D_{it} of $7\times 10^{12}\,\mathrm{eV}^{-1}\,\mathrm{cm}^{-2}$ for oxidized samples in O_2 at 900 °C for 6 min have been reported along with a fixed oxide charge density of approximately $1.0\times 10^{11}\, q/\mathrm{cm}^{-2}$ for oxidation in O_2 at 750 °C.[30]

IV. SUMMARY AND CONCLUSIONS

Rapid thermal oxidation of Si in pure O_2 and O_3 (950 ppm)/O_2 environments has been studied at temperatures between 200 and 550 °C. *In situ* mirror-enhanced reflection FTIR spectroscopy has been used to monitor changes in the frequency and intensity of all IR spectral features, and, thus, the thickness and properties of ultrathin (<30 Å) SiO_2 films. The oxidation rate of Si (100) by ozone is shown to be higher than that by pure oxygen; in fact, oxidation in ozone is found to be as active as oxidation in pure O_2 at about 200 °C higher. The enhancement factor [i.e., oxidation rate in O_3 (950 ppm)/O_2 over oxidation rate in pure O_2] initially increases with temperature, but it starts decreasing at a temperature between 400 and 500 °C. Data analyses suggest a fast oxidation rate regime early on, followed by a slow one, the activation energies of which are about 0.13 and 0.19 eV, respectively, in ozone, and 0.20 and 0.36 eV, respectively, in pure oxygen ambient. These findings are consistent with the proposition that oxidation in the presence of ozone proceeds primarily via atomic oxygen.

The IR spectral shifts in ozone and pure O_2 gas feeds can be explained primarily in terms of stoichiometry along with a likely small contribution from strain/stress at the interfacial layer. At each oxidation temperature, the LO mode of Si–O–Si asymmetric stretching of an ozone-oxidized sample is found to be at higher wavenumbers than that of a pure O_2-oxidized one. Quantification of the amount of suboxide in the films with XPS corroborates the proposition that smaller amounts of suboxide in the interfacial layer are mostly responsible for the higher frequencies of ozone-treated substrates. Preliminary electrical characterization suggests that oxides formed in ozone ambient are of higher quality than those formed in pure molecular oxygen.

ACKNOWLEDGMENTS

The authors are grateful to Semitest. Inc., especially Valerie Chapman, for supporting this work by providing all electrical characterizations. They owe many thanks to Rick Haasch from the University of Illinois at Urbana-Champaign for the XPS data. Funding by the National Science Foundation (NSF) is also acknowledged.

[1] G. D. Wilk and B. Brar, IEEE Electron Device Lett. **20**, 132 (1999).
[2] A. Kazor, R. Gwilliam, and I. W. Boyd, Appl. Phys. Lett. **65**, 412 (1994).
[3] K. Nakamura, S. Ichimura, A. Kurokawa, K. Koike, G. Inoue, and T. Fukuda, J. Vac. Sci. Technol. A **17**, 1275 (1999).
[4] A. Kazor and I. W. Boyd, Appl. Phys. Lett. **63**, 2517 (1993).
[5] I. W. Boyd, V. Cracium, and A. Kazor, J. Appl. Phys. **32**, 6141 (1993).
[6] S. C. Chao, R. Pitchai, and Y. H. Lee, J. Electrochem. Soc. **136**, 1251 (1989).
[7] H. Ono, T. Ikarashi, K. Ando, and T. Kitano, J. Appl. Phys. **84**, 6064 (1998).
[8] R. A. B. Devine, Appl. Phys. Lett. **68**, 3108 (1996).
[9] J. T. Fitch, C. H. Bjorkman, G. Lucovsky, F. H. Pollak, and X. Yin, J. Vac. Sci. Technol. B **7**, 775 (1989).
[10] Y. Ishikawa, T. Shibamoto, and I. Nakamichi, Jpn. J. Appl. Phys., Part 1 **31**, 1148 (1992).
[11] Z. Cui and C. G. Takoudis (unpublished).
[12] Z. H. Lu and M. J. Graham, Appl. Phys. Lett. **63**, 2941 (1993).
[13] F. J. Himpsel, F. R. McFeely, A. Taleb-Ibrahimi, J. A. Yarmoff, and G. Hollinger, Phys. Rev. B **38**, 6084 (1988).
[14] C. M. Kohn and W. C. Goldfarb, Solid State Technol. **38**, 93ff (1995).
[15] B. Harbecke, B. Heinz, and P. Grosse, Appl. Phys. A: Solids Surf. **38**, 263 (1985).
[16] K. Krishnan, P. J. Stout, and M. Watanabe, in *Practical Fourier Transform Infrared Spectroscopy: Industrial and Laboratory Chemical Analysis*, edited by J. R. Ferraro and K. Krishnan (Academic Press, San Diego, 1990), p. 285.
[17] A. Kazor and I. W. Boyd, Electron. Lett. **29**, 115 (1993).
[18] J. M. Madsen, Z. Cui, and C. G. Takoudis, J. Appl. Phys. **87**, 2046 (2000).
[19] O. M. R. Chyan, J. Wu, and J. Chen, Appl. Spectrosc. **51**, 1905 (1997).
[20] C. R. Chen, S. F. Hu, P. C. Chen, H. L. Hwang, and L. C. Hsia, J. Vac. Sci. Technol. B **16**, 2712 (1998).
[21] A. Reisman, E. H. Nicollian, K. C. Williams, and C. J. Merz, J. Electron. Mater. **16**, 45 (1987).
[22] H. Watanabe, K. Kato, T. Uda, K. Fujita, M. Ichikawa, T. Kawamura, and K. Terakura, Phys. Rev. Lett. **80**, 345 (1998).
[23] E. P. Gusev, H. C. Lu, T. Gustafsson, and E. Garfunkel, Phys. Rev. B **52**, 1759 (1995).
[24] I. Trimaille, F. C. Stedile, J.-J. Ganem, I. J. R. Baumvol, S. Rigo, and E. P. Gusev, *The Physics and Chemistry of SiO_2 and Si-SiO_2 Interface* (Electrochemical Society, Pennington, NJ, 1996), Vol. 3, p. 59.
[25] T. Hoshina, M. Tsuda, S. Oikawa, and I. Ohdomari, in *Control of Semiconductor Interfaces*, edited by I. Ohdomari, M. Oshima, and A. Hiraki (Elsevier, Amsterdam, 1994), p. 221.
[26] J. A. Moreno, B. Garrido, J. Samitier, and J. R. Morante, J. Appl. Phys. **81**, 1933 (1996).
[27] M. Nakamura, Y. Mochizuki, K. Usami, Y. Itoh, and T. Nozaki, Solid State Commun. **12**, 1079 (1984).
[28] H. Ono, T. Ikarashi, and A. Ogura, Appl. Phys. Lett. **72**, 2853 (1998).
[29] Y. Ishikawa, T. Shibamoto, and I. Nakamichi, Jpn. J. Appl. Phys., Part 1 **31**, 1148 (1992).
[30] J. Ruzyllo, P. Roman, D. O. Lee, M. Brubaker, and E. Kamieniecki, Proc. SPIE **3884**, 198 (1999).